Available online at http://bajas.edu.iq
https://doi.org/10.37077/25200860.2022.35.2.10
College of Agriculture, University of Basrah

Basrah Journal of Agricultural Sciences

ISSN 1814 – 5868 Basrah J. Agric. Sci., 35(2), 132-159, 2022 E-ISSN: 2520-0860

Antibacterial and Anticancer Effects of Silver Nanoparticles Synthesised using *Eragrostis tef* and *Vitellaria paradoxa* Seeds Extract

Suha M. A. Almudhafar* & Maytham A. Al-Hamdani
Department of Biology, College of Pure Science, University of Basrah, Iraq

***Corresponding author email:** suha.almudhafar@gmail.com, (M.A.A.): maytham.abdulkadir@uobasrah.edu.iq

Received 12th April 2021; Accepted 18th October 2021; Available online 13th October 2022

Abstract: The present study aims to investigate the biosynthesis of silver nanoparticles using the aqueous extract of the *Eragrostis tef* (teff or annual bunch grass) and *Vitellaria paradoxa* (Shea Butter Tree) seeds extract and investigate their antimicrobial and anticancer activities. In order to synthesise the silver nanoparticles, aqueous extract of the plant was prepared and introduced into a 1mM silver nitrate solution. The synthesised AgNPs were characterised using various instrumental techniques including ultraviolet-visible spectroscopy, Fourier transformed infrared spectroscopy (FTIR), scanning electron microscope (SEM). Surface Plasmon Resonance (SPR) for AgNPs using *E. tef* and *V. paradoxa* seeds extract was observed at 40 nm. The synthesised AgNPs of *E. tef* and *V. paradoxa* was found with diameter of 12.59- 34.60 nm, 29.05- 83.94 nm respectively. The antibacterial result against the experimental pathogens was found to range from 12-22 mm and from 13-19 mm using AgNPs of *E. tef*, *V. paradoxa* seed extracts respectively. In addition the result show that there was clear effect on *Acinetobacter baumannii* from hospital sewage isolates. Toxic effect of AgNPs against cancer cell were 77.12 (concentration of AgNPs was 75%) of *E. tef* and 77.23 (concentration of AgNPs was 50%) of *V. paradoxa*.

Keywords: Anticancer, Green synthesis, Pathogenic bacteria, Silver nitrate.

Introduction

Nanotechnology is an important area of modern research that deals with the synthesis, strategy, and manipulation of particle structure with a size of ~1 to 100 nanometers. Within this size range, all propertiZes (chemical, physical and biological) change in ways fundamental to both individual atoms/molecules and their corresponding mass. New applications of nanoparticles and nanomaterials are proliferating on different fronts due to their completely new or enhanced properties based on size, distribution, and morphology. It is gaining rapid innovation in a large number of fields such as healthcare, cosmetics, biomedicine, food and feed, pharmaceutical gene delivery, environment, health, mechanics, optics, chemical industries, electronics, aerospace industries, energy and catalysis sciences, light emitters, single-electronic transistors, nonlinear optical devices and optoelectrochemical applications (Ahmed *et al*., 2016). The tremendous growth in these expanding technologies had opened applied frontiers and novel fundamentals. This includes the production of nanoscale materials afterwards in investigation or utilisation of their mysterious physicochemical and optoelectronic properties (Kaviya &

Viswanathan, 2011; Korbekandi & Iravani, 2012; Khalil *et al*., 2013).

Metal nanoparticles are among the most promising because they have amazing antibacterial properties due to their large surface area to volume ratio, which is of interest to researchers due to the increasing microbial resistance against antibiotics and the development of resistant strains (Khalil *et al*., 2013). Among all the metallic nanoparticles, silver nanoparticles are a product from the field of nanotechnology that has increased its unlimited interests due to its sole properties such as chemical stability, good conductivity, catalyst, the most important of which are antibacterial, antiviral, antifungal affects, as well as anti-inflammatory activities which They can be incorporated into cryogenic highly conductive materials, cosmetic products, the food industry, and electronic components (Klaus-Joerger *et al*., 2001; Ahmed *et al*., 2003).

Ag NPs target both the respiratory chain and the cell division machinery, while simultaneously releasing silver ions (Ag^{+}) that enhance the bactericidal activity, ultimately leading to cell death (Prabhu & Poulose, 2012). The antimicrobial activity of Ag NPs depends on their sizes (Lu *et al*., 2013) and shape (Pal *et al*., 2007).Using AgNPs for cancer therapy are an affordable way to control tumor growth and constitute a choice strategy to fight cancer cells (Al-Musawi & Al-Saadi, 2021).

Plants are preferred for the synthesis of Ag NPs over other biological processes for several reasons; i- It is less expensive, ii- It can be properly expanded for large-scale NP synthesis, iii-Using plant for nanoparticles can be advantageous over other biological processes by eliminating the elaborate process of maintaining cell culture because some chemical methods cannot avoid the use of toxic chemicals in the synthesis protocol. Furthermore, biological methods of nanoparticles synthesis using microorganisms or enzymes (Satyavani *et al*., 2011) and iv-plant extracts contain many antioxidants, which act as reducing agents and capping agents (Mittal *et al*., 2013).

Emergence and spread of carbapenem-resistant Enterobacteriaceae (CRE) is a major clinical and public health concern. Beta-lactams are often the primary treatment option for serious infections, and carbapenems, in particular, are often considered agents of last choice. Thus, CRE is often resistant to all beta-lactam drugs and often carries mechanisms that discuss resistance to other classes of antimicrobials, further underestimating treatment options. Although bad bacteria are rare, they have become more common in the United States since their emergence (Gupta *et al*., 2011; Guh *et al*., 2014; Vasoo *et al*., 2015). Numerous studies indicate the prevalence of multi-resistant pathogens (Al-Hamdani & Abas, 2013; Al-Hamdani *et al*., 2020).

Infections with these resistant bacteria is associated with higher mortality rates than those caused by organisms exposed to carbapenems (Esterly *et al*., 2012). Many different stakeholders are interested in detecting carbapensemase-producing CRE (CP-CRE), which is useful at the clinical, local, regional and national levels. Detection is essential for clinicians treating patients with this infection and for infection owners and regional prevention relations trying to limit the spread of these organisms, and a coordinated approach to germ prevention has also been recently highlighted, with all regional stakeholders involved in CRE prevention knowing about the spread of CRE , has the option to bring about significant reductions in HIV transmission compared to traditional

single-institution-based approaches (Slayton *et al*., 2015).

Since the antibacterial effect of medicinal plants varies greatly depending on the phytochemical properties of the plant families and subfamilies, it is not surprising to note the difference in this efficacy even when using samples taken from the same plant, but from two different regions (Sarac & Ugur, 2009).

Naturally, these plants were used as herbal medicines.The plant is a diuretic and anti-inflammatory and treats digestive diseases, carminative, tonic, and puerperal. The whole *P. murex* plant is used as a medicine for stomach pain, headache, diarrhea, dysentery, Microorganisms were obtained from some hospitals of Basrah. These microorganisms were collected from two resources, the first cough and cold, intestinal infections, (Anandalakshmi *et al*., 2016). The plants used in this study are *E. tef* (Teff) and *V. paradoxa* (Shea butter tree) are medicinal and beneficial to humans, and their seeds were selected for this study as there are no previous studies on them. This study aims to study the antibacterial effect of the prepared nanoparticles, to investigate the mechanisms of the prepared nanoparticles as an antibacterial, and to study the toxicity of the prepared nanoparticles on the eukaryotic cell (cancer cells).

Materials & Methods

Microorganisms

once was collected during September 2019 to December 2019 from patients of some hospitals in Basrah as shown in table (1).

Table (1): The first type of isolates from patients (pathological isolates).

Date	Name of hospital	Select organisms
Sep 25,2019	General Basrah Hospital	*Proteus mirabilis*
Sep 24,2019	General Basrah Hospital	*Psuedomonas aeruginosa*
Sep 25,2019	Al-Fayhaa General Hospital	*Proteus mirabilis*
Sep 25,2019	Al-Fayhaa General Hospital	*Proteus mirabilis*
Oct 20,2019	Al-Fayhaa General Hospital	*Klebsiella pneumonia* ssp. *ozaenae*
Oct 20,2019	Al-Fayhaa General Hospital	*Acinetobacter baumannii* complex
Nov 4,2019	Al-Fayhaa General Hospital	*Psuedomonas aeruginosa*
Nov 7,2019	Ibn Ghazwan Maternity and Pediatrics Hospital	*Acinetobacter baumannii*
12, Nov 2019	Al-Fayhaa General Hospital	*Acinetobacter baumannii*
Nov 12,2019	Al-Fayhaa General Hospital	*Klebsiella pneumoniae* ssp. *Pneumonia*
Nov 21,2019	General Basrah Hospital	*Klebsiella pneumoniae* ssp. *pneumonia*
Nov 26,2019	General Basrah Hospital	*Klebsiella pneumoniae* ssp. *pneumonia*
Nov 27,2019	Al-Fayhaa General Hospital	*Acinetobacter baumannii* Complex
Dec 2,2019	Al-Fayhaa General Hospital	*Acinetobacter baumannii*
Dec 24,2019	Al-Fayhaa General Hospital	*Psuedomonas aeruginosa*
Dec 24,2019	Al-Fayhaa General Hospital	*Acinetobacter baumannii*
Dec 24,2019	Ibn Ghazwan Maternity and Pediatrics Hospital	*E. coli*

The second resource of isolates were collected from Al-Fayhaa hospital sewage. The isolates were identified using Vitek® 2 system, sensitivity information presented in table (2).

Table (2): Sensitivity information of bacterial isolates.

Organism	Antibiotic	Susceptibility	MIC
Enterobacter cloacae ssp. *dissolvens*	Imipenem	Sensitive	2
	Meropenem	Resistant	>=16
Raoultella ornithinolytica	Imipenem	Sensitive	<=0.25
	Meropenem	Sensitive	<=0.25
Acinetobacter baumannii	Imipenem	Sensitive	<=0.25
	Meropenem	Sensitive	<=0.25
Escherichia coli	Imipenem	Sensitive	2
	Meropenem	Sensitive	0.5
Enterobacter aerogenes	Imipenem	Sensitive	2
	Meropenem	Sensitive	0.5

Preparation of the extracts

Two types of plants include seeds of *Eragrostis tef*, *Vitellaria paradoxa* were used to make the aqueous extract. The extracts were prepared by using 5 g of washed and powdered seeds and mixed with 100 ml of deionised water in a 500 ml Erlenmeyer beaker and then boiling the mixture for 10 minutes before finally decanting it and filtered the mixture through it Whatman No. 1 filter paper (pore size 25 micrometers). (Saxena *et al*., 2010; Singh *et al*., 2010).

Gas Chromatography-Mass spectrometry (GC-Ms)

GC-MC is widely used in the medical industries for analytical research and development, quality control, quality assurance, production, and pilot plant divisions for active pharmaceutical ingredients (API), bulk drugs and formulations. It is an integral part of research related to medicinal chemistry (synthesis and characterisation of compounds), pharmaceutical analysis (stability testing, impurity identification), pharmaceutical process control, and pharmaceutical biotechnology. (Al- Rubaye *et al*., 2017). In this study the powder of seeds extracts was dried. 20g of powder was soaked in methanol, then put in oven temperature 300°C with slow fan for 1 min then 60°C for 10 min then 10°C/min to 280°C for 3, the run time was 35 min. The samples were examined by Gas Chromatography-Mass Spectrometry (GC-MS).

Synthesis of silver nanoparticles

A 2mM aqueous solution of silver nitrate ($AgNO_3$) was prepared and used for the synthesis of silver nanoparticles. This aqueous solution was prepared by dissolving 0.39 g of silver nitrate in a liter of deionized distilled water. 10 mL of the plant extract was added to 90 mL of a 2mM aqueous solution of silver nitrate for reduction to Ag^+ ions and kept at room temperature for 4 h (Singh *et al*., 2010).

Ultra Violate Visible spectroscopy (UV-Vis)

Reduction of pure Ag^+ ions was verified by UV-Vis spectrometry of the reaction medium by UV-visible spectrophotometry. This means that it uses light in the visible and adjacent

bands (near ultraviolet and near infrared (NIR). Absorption in the visible range directly affects the apparent color of the chemicals involved. In this region of the electromagnetic spectrum, molecules undergo electronic transitions. (Saxena *et al*., 2010). The spectrum was recorded with a range of 300-800 nm, and the wavelength corresponding to the maximum absorption at room temperature was determined.

Fourier Transform Infrared Spectroscopy (FTIR)

The remaining 30 mL solution after reaction was centrifuged at 10,000 rpm for 10 min. The resulting suspension was added in 2 mL sterile distilled water, to remove any free biomass residue or a compound that is not a covering ligand for the nanoparticles, the process was repeated three times. Then, the purified suspension was freeze-dried to obtain a dried powder. The dried samples were mixed in a slurry with KBr and pressed into disks. (Singh *et al*. 2010) In the final stage, the FTIR spectra were recorded at room temperature and the dried nanoparticles were analysed by FT-IR-4200 JASCO/Japan.

7- SEM analysis of silver nanoparticles

Scanning Electron Microscopy (SEM) analysis is a testing process that scans a sample using an electron beam to produce an enlarged image of sample for analysis. Thin films of the sample (AgNPs prepared from plant extracts) were added onto a carbon-coated copper grid by dropping a very small amount of the sample onto the grid, the additional solution was removed using blotting paper and then the film on the SEM The grid was allowed to dry by placing it under a mercury lamp for 5 minutes. Finally, samples were examined by SEM. (Singh *et al*., 2010). In Field Emission Scanning Electron Microscopy (FESEM), electron beams emits by a field emission electron gun and is focused by electromagnetic lenses on the surface of sample. These electrons are incident onto the surface of the sample resulting various signals containing the emission of electrons and photons from the surface of the sample. Elastic collision causes high energy electrons while inelastic collision produces secondary electrons. The secondary electrons are collecting by the detector to obtain an image of the sample surface.

Antibacterial activity by well diffusion method

Silver nanoparticles (AgNPs) were synthesised in seeds extract of *Eragrostis tef*, and *Vitellaria paradoxa*, the synthesised particles were tested for their antibacterial activity by good diffusion method against pathogenic organisms including 17 isolates, and from wastewater from Al Fayha Hospital including 16 isolates. The pure culture of the organism was cultured on nutrient agar. Each strain was uniformly wiped on the individual plates using a sterile cotton swab. 6 mm wells were made on Muller-Hinton agar plates using a gel puncture. Using a micropipette 50 µL of nanoparticles (silver nitrate AgNO3 with plant extracts), and $AgNO_3$ solution sample without plant extracts, and plant extracts were poured into the wells on all dishes. After incubation at 37 °C for 18 h, the different levels of the inhibition zone were measured (Logeswari *et al*., 2015).

Anticancer activity

Maintenance of cell cultures

Human Breast Cancer Cell Line MCF-7 & human mammary cell line HBL100 were obtained from the Iraq Biotechnology Cell Bank unit in Basra and maintained in RPMI-1640 supplemented with 10% fetal bovine, 100 units.ml^{-1} penicillin and 100 µg.ml^{-1} streptomycin. Cells were passaged with

trypsin-EDTA re-seeded at 50% confluence twice a week and incubated at 37 °C (Al-Shammari *et al*. 2015).

To determine the cytotoxic effect of the nanoparticles, MTT cell viability assay was performed on 96-well plates. MCF7 and HBL100 cell lines were seeded at density of 1 × 10^4 cells.well^{-1}. After 24 h or confluent monolayers, cells were treated with the tested compounds (A: *E*. *tef* and B: *V*. *paradoxa*) at a final concentration (AgNPs 50, 75, extracts 50, $AgNO_3$ 50) µg.ml^{-1}. Cell viability was measured after 72 hours of incubation. From treatment by removing the medium, add 28 µl of 2 mg.ml^{-1} MTT solution and incubate the cells for 2 h at 37 °C after removing the MTT solution, the crystals remaining in the wells were dissolved by adding 100 µL of DMSO (dimethyl Sulphoxide) followed by incubating 37°C for 15 min with shaking (Al-Shammari *et al*. 2019), the absorbance was determined on a microplate reader at 620 nm (test wavelength); the assay was performed in triplicate. The rate of cell growth inhibition (percentage of cytotoxicity) was calculated with the following equation:

Proliferation or diffusion rate (PR) = $B/A * 100$ where A is the average optical density of Untreated wells, B is the optical density of treated wells and inhibition rate (IR) = 100- PR (Freshney, 2010).

Statistical analysis

In this paper the Least of Standard Deviation (LSD) are used to analyse the results. All experiments were done in duplicate and then values were expressed as mean ± standard deviation (SD). Statistical significance (5%) was evaluated by one-way analysis of variance (ANOVA) ($p < 0.05$, SPSS 11 version).

Results & Discussion

Comparative of Susceptibility between two types of isolates

Using the Vitek®2 chart report, a comparison sensitivity information was made on the two resources of isolates (type 1 from hospital laboratories and type 2 from hospital wastewater) against antibiotics (Table 3).

The results showed that most isolates of the first type were resistant to carbapenems, while the second isolates were sensitive. In Iraq, several studies on carbapenem-resistant bacteria were conducted in April to October, the study was conducted in the city of Sulaymaniyah. Total meropenem resistance in this study was 22% of Gram-negative bacteria (Anoar *et al*., 2014). In 2008 a study was conducted in Baghdad. The overall resistance to imipenem in this study was 20% *Pseudomonas auruginosa* (Al-Marjani *et al*. 2010). Manoharan *et al*. (2011) reported 17% resistance to carbapenems in *Enterobacteriaceae*. It also showed (Gupta *et al*., 2006; Dutta *et al*. 2012) resistance of 7.87% and 17.22% to carbapenems, respectively.

GC-Mass

Exploration of phytochemical screening using methanol extracts of *Eragrostis tef* and *Vitellaria paradoxa* revealed the presence of phytochemical components as shown in table (4). The compounds present in the methanolic extract of *Eragrostis tef*, were identified by GC-MS analysis (Fig. 1). The active principles in *Eragrostis tef* seed extract with retention time (RT), concentration (%), name of compounds, the compounds present in the methanolic extract of Vitellaria paradoxa were identified by GC-MS analysis (Fig. 2). molecular formula, and molecular weight (MW), are presented in table (5)

Table (3): Comparative of susceptibility between two types of isolates.

Bacterial isolates (Type 1)	Resistance (%)	Intermediate (%)	Sensitive (%)	Bacterial isolates (Type 2)	Resistance (%)	Intermediate (%)	Sensitive (%)
P. mirabilis	76.48	11.76	11.76	*E. cloacae* ssp. *dissolvens*	71.40	14.30	14.30
P. aeruginosa	73.33	0	26.67	*R. ornithinolytica*	0	7.10	92.90
A. baumannii	93.75	0	6.25	*A. baumannii*	16.67	8.33	75
K. pneumonia ssp. *pneumonia*	72.22	16.67	11.11	*E. aerogenes*	14.30	0	85.70
E. coli	64.30	0	35.70	*E. coli*	0	0	100

Table (4): Phytochemical constituents present in methanolic extracts.

Plant extracts	Phytochemicals	References
Eragrostis tef	1) Phenols, Flavonoids	Boka *et al*, 2013
Vitellaria paradoxa	1) Alkaloid, Saponin, Tannin and Phytate contents	Animasaun *et al*, 2019

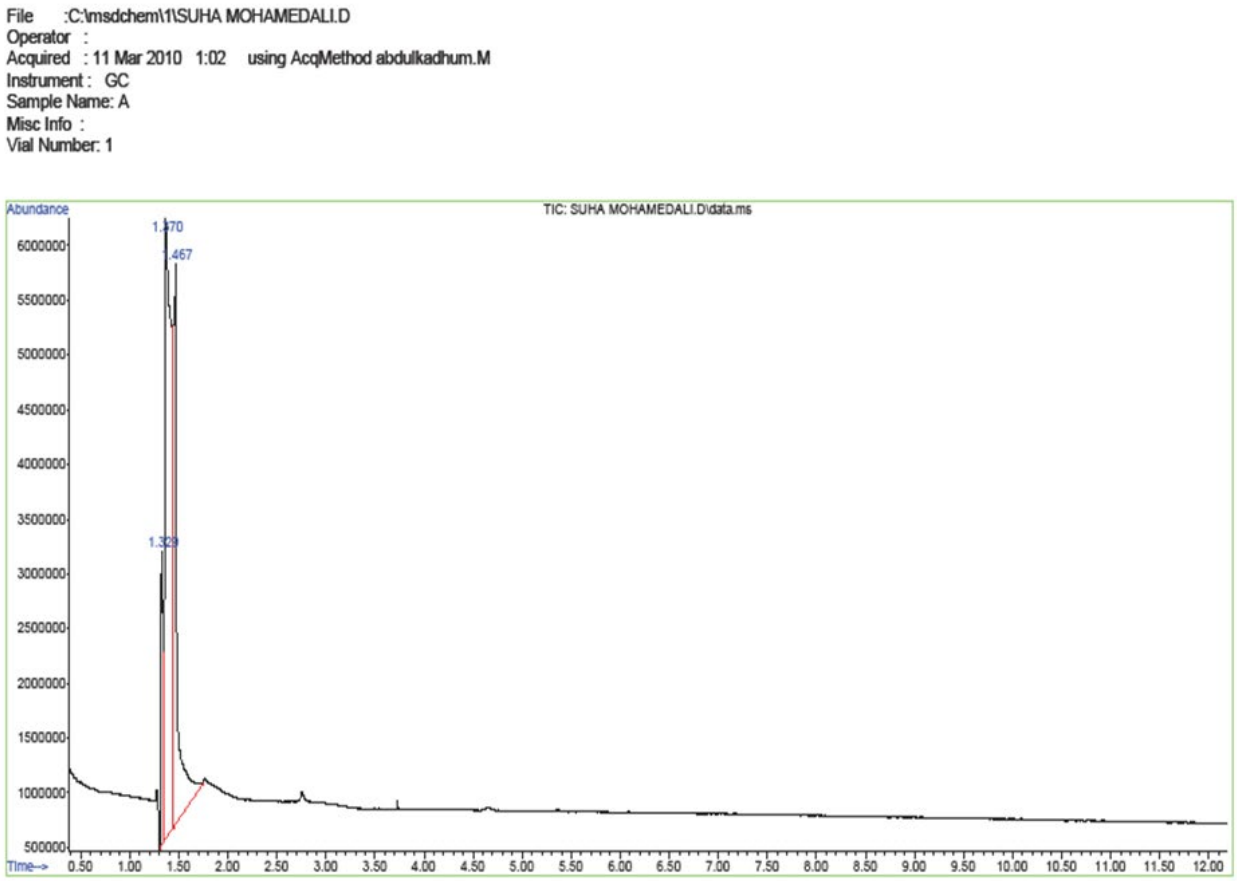

Fig. (1): GC-MC analysis of *Eragrostis tef* seed extract.

Table (5): Phytocomponents identified in the methanolic extract of the *Eragrostis tef* seeds.

S. No.	RT	Area%	Name of compound	Molecular formula	MW ((g.mole^{-1})
1	1.32	2.36	Acetaldehyde, hydroxy-	CH_3CHO	44.05
2	1.32	1.47	Glycolaldehyde dimer	$C_4H_8O_4$	120.10
3	1.32	1.07	Methyl formate	$C_2H_4O_2$	60.05
4	1.32	0.78	Hydroxyacetic acid, hydrazide	$C_2H_6N_2O_2$	90.08
5	1.32	0.42	Hydrazine	N_2H_4	50.06
6	1.32	0.39	Acetic acid, hydroxy-	CH_3COOH	60.05
7	1.32	0.26	Acetic acid, oxo-, methyl ester	$C_3H_4O_3$	88.0621
8	1.37	6.93	Acetic acid, hydroxy-	CH_3COOH	60.052
9	1.37	4.61	Acetic acid, ethoxyhydroxy-, ethyl ester	$C_9H_{20}O_4Si$	220.34
10	1.37	0.75	Ethyl formate	$C_3H_6O_2$	74.08
11	1.37	0.29	Ethanol, 2-fluoro-	C_2H_5FO	64.0589
12	1.37	0.26	Methyltartronic acid	$C_4H_6O_5$	134.09
13	1.37	0.25	Acetic acid, hydroxy-, ethyl ester	$C_4H_8O_3$	104.1045
14	1.47	2.65	Acetic acid, hydroxy-	CH_3COOH	60.052
15	1.47	2.55	Acetic acid, ethoxyhydroxy-, ethyl ester	$C_9H_{20}O_4Si$	220.34
16	1.47	0.53	Methyltartronic acid	$C_4H_6O_5$	134.09
17	1.47	0.40	Ethyl formate	$C_3H_6O_2$	74.08
18	1.47	0.22	Ethanol, 2-nitro-	$C_2H_5NO_3$	91.07
19	2.85	39.6	1-Benzylbenzimidazole 3-oxide	$C_{14}H_{12}N_2O$	224.258
20	2.85	9.41	Benzene, 1-chloro-2-(phenylmethoxy)-	$C_{13}H_{11}ClO$	218.679
21	2.85	7.58	4-Azido-2-phenylmethanesulfinyl-benzonitrile	$C_{14}H_{10}N_4OS$	282.3204
22	2.85	6.70	Butanoic acid, 3-methyl-2-[(phenylmethoxy)imino]-, trimethylsilyl ester	$C_{15}H_{23}NO_3Si$	293.43
23	2.85	3.26	Carbamic acid, (4-nitrophenyl)-, phenylmethyl ester	$C_{14}H_{11}N_2O_4$	271.25
24	5.2	30.7	Hydroxyacetic acid, hydrazide	$C_2H_4O_3$	76.05
25	5.2	21.7	Carbon monoxide	CO	28.01
26	5.2	8.57	Butanenitrile, 2,3-dioxo-, dioxime, O,O'-diacetyl-	$C_8H_9N_3O_4$	167.126
27	5.2	5.36	Nickel tetracarbonyl	$Ni(CO)_4$	170.73
28	5.2	4.53	4-Methyl-3,4-dihydro-[1,2,3]triazolo[4,5-d]pyrimidine-5,7-dione	$C_5H_5N_5O_2$	167.126
29	5.2	4.18	Nitrogen	N	14.0067
30	5.2	4.18	Acetic acid, hydrazide	$C_2H_6N_2O$	74.0818
31	8	36.9	Hydroxyacetic acid, hydrazide	$C_2H_4O_3$	76.05
32	8	12.4	Carbon monoxide	CO	28.01
33	8	9.97	Butanenitrile, 2,3-dioxo-, dioxime, O,O'-diacetyl-	$C_8H_9N_3O_4$	211.170
34	8	8.42	4-Methyl-3,4-dihydro-[1,2,3]triazolo[4,5-d]pyrimidine-5,7-dione	$C_5H_5N_5O_2$	167.126
35	8	4.60	Nickel tetracarbonyl	$Ni(CO)_4$	170.73
36	8	3.70	Acetic acid, hydrazide	$C_2H_6N_2O$	74.0818

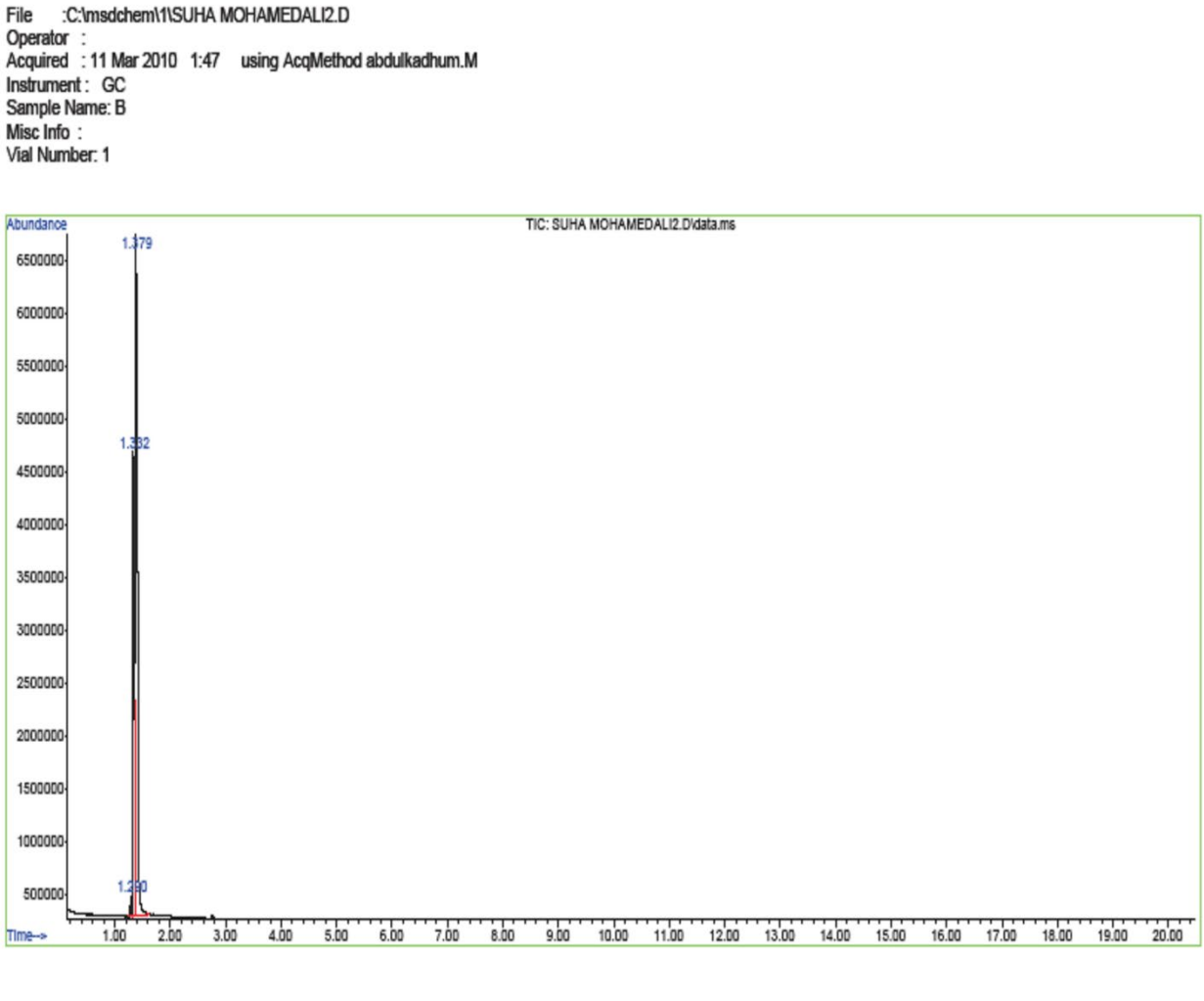

Fig. (2): GC-MC analysis of *Vitellaria paradoxa* seed extract.

The active principles in *Vitellaria paradoxa* seeds extract with their retention time (RT), concentration (%), name of compounds, molecular formula, and molecular weight (MW), are presented in table (6). The present research work dealt with methanol extracts of plant seed extract of *E. tef* and *V. paradoxa* for gas chromatography-mass spectrometry analysis. GC-MS analysis of a study (Santhosh *et al*., 2014) showed that the presence of a major compounds such as 5-7A-Isoprpenyl-4, 5-dimethyloctahydro-1h-inden-4yl-3-methyl-2-penta, (24.49%), nexadecanoic acid (18.29%), gamma-sitosterol (10.61%).

Table (6): Phytocomponents identified in the methanolic extract of the *Vitellaria paradoxa* seeds.

S. No.	RT	Area (%)	Name of compound	Molecular formula	MW (g.mole^{-1})
1	1.29	49.1	(2-Aziridinylethyl)amine	$C_4H_{10}N_2$	86.14
2	1.29	22.4	Benzeneethanamine, 3-fluoro-β,5-dihydroxy-N-methyl-	$C_9H_{12}FNO_2$	185.198
3	1.29	6.34	(R)-(-)-2-Amino-1-propanol	C_3H_9NO	75.11
4	1.29	4.85	Phenethylamine, p,α-dimethyl-	$C_{14}H_{23}N$	205.34
5	1.29	4.29	3-Methoxyamphetamine	$C_{11}H_{17}NO$	179.263
6	1.29	3.96	Dextroamphetamine	C_9NH_{13}	135.2062
7	1.29	3.11	Hydroxyurea	$CH_4N_2O_2$	76.055
8	1.33	2.84	Acetaldehyde, hydroxy-	C_2H_4O	44.05
9	1.33	0.77	Methyl formate	$C_2H_4O_2$	60.05
10	1.33	0.56	Hydrazine	N_2H_4	32.05
11	1.33	0.54	Glycolaldehyde dimer	$C_4H_8O_4$	120.10
12	1.37	2.62	Acetic acid, hydroxy-	C_2H_4O	76.0514
13	1.37	2.42	Acetic acid, ethoxyhydroxy-, ethyl ester	$C_6H_{12}O_4$	148.16

Table (7): Active of phyto-components identified in plant extracts by GC-MC.

Plant extract	RT	Area (%)	Name of compound	Activity
Eragrostis tef	1.32	2.36	Acetaldehyde	Pharmacological properties, stimulation and reinforcement that are characteristic of addictive drugs
Eragrostis tef	1.37	6.93	Acetic acid	Antibacterial activity
Eragrostis tef	2.85	39.6	1-Benzylbenzimidazole 3-oxide	Anti-inflammatory activity, a risk factor for a host of chronic diseases such as autoimmune disorders, neurodegenerative disorders and cancer
Eragrostis tef	5.2	30.7	Hydroxyacetic acid	Antibacterial activity
Vitellaria paradoxa	1.29	49.1	(2-Aziridinylethyl)amine	Useful intermediate used to synthesise aminopropyl dihydrogen phosphate, used to prepare 17-aminogeldanamycin derivatives with possible antitumor activity

Bioactive compounds such as gamma-sitosterol, vaquinic acid, octadecanoic acid, phytol, squalene, hexaethylene glycol monodecyl ether, hydroquinine, 9-octadecinamide, 15-hydroxypentadecanic acid, Cis-Vaccenic acid, and cis-9-Hexadecan. Compounds including vitamin E are also present. The GC-MS chromatogram of the

seven peaks of the compounds was revealed. GC-Ms chromatogram analysis of the methanol extract of *Adiantum capillus-veneris* showed the presence of 3 main peaks and the corresponding components of the peaks were identified. Many medicinal plants are a rich source of secondary metabolites such as alkaloids, phenols, cardiac glycosides, flavonoids, tannins and terpenoids determined by gas chromatography and mass spectrometry (Lewis & Ausubel, 2006; Adekunle & Adekunle, 2009). Kumar *et al*. (2010) also reported that the activities of some plant components of synthesized nature of flavonoids, palmitic acid (hexadecanoic acid, ethyl ester, nexadeconic acid), polyunsaturated fatty acids and linoleic acids (DPA and OCTA) as antimicrobial, anti-inflammatory, antioxidant, hypocholesterolemic, and cancer prevention, Hepatoprotective, anti-inflammatory, antihistamine, anti-blood and anti-crohn's. Identified squalene also contains hydrocarbon derivatives and a triterpene that has antioxidant properties and chemopreventive activity against colon carcinogenesis (Kala *et al*., 2011).

Bharati *et al*. (2012) analysed that Vitol is a diterpene with antimicrobial properties, significantly against several bacterial strains. Among the plant compounds identified Dodecanoic acid, tetrdecanoic acid and n-Hexadecanoic acid possess antioxidant and antimicrobial activities (Bodoprost & Rosemeyer, 2007). Terpenoids are an important compound of volatile substances from plants. Most of them have different chemical functions in the allele. Carthamus lanatus has been identified as two sesquiterpenes, α-bisabolol, caryophyllene oxide and α-Bisabolol fucopyranoside are the main components analyzed by gas chromatography and mass spectrometry (Feliciano *et al*., 1990). Balaji *et al*. (2014) reported that GC-MS analysis of different extracts from the leaves of clerodendrum phlomidis. Grover & Patni (2013) also reported that GC-MS analyses of the methanolic extract of woodfordia fruticosa twenty-one compounds were identified.

FTIR

To investigate the Ag-bound nanoparticles, FTIR measurements were performed. The Ag nanoparticle solution (100 ml) was centrifuged at 5000 rpm for 20 min. The pellets were washed three times with 10 mL of de-ionised water to eleminate the free proteins/enzymes not covering the silver nanoparticles. Samples were dried, ground with potassium bromide (KBr) and analysed on a Japan-made JASCO FT/IR-4200 model in diffuse reflection mode operating at 4 cm^{-1} resolution. The FTIR spectrum results for *E*. *tef* and *V*. *paradoxa* are shown in figs. (3 and 4).

FT-IR analysis of *E*. *tef* seeds extract showed that the appearance of a peak at 3,429 cm^{-1} which is correlates with the NH stretching bond of the primary aromatic amines. The peak at 2926 cm^{-1} is due to the C-H stretching of methylene. The band at 1655 cm^{-1} is due to the C = C stretch of the alkenyl. The bar at 1539 cm^{-1} indicates the presence of aromatic nitro compounds. The range at 1424 cm^{-1} indicates the carbonate ion the band at 1374 cm^{-1} C-H methyl curve.

The 1157 cm^{-1} band indicates the CN extension of the secondary amine. The band at 1021 cm^{-1} indicates the CN extension of the primary amine. Both bands 762,705 cm^{-1} indicate the C-Cl stretch of aliphatic chloro compounds. Moreover, both 572 and 527 cm^{-1} bands indicate the C-I stretch of aliphatic iodine compounds.

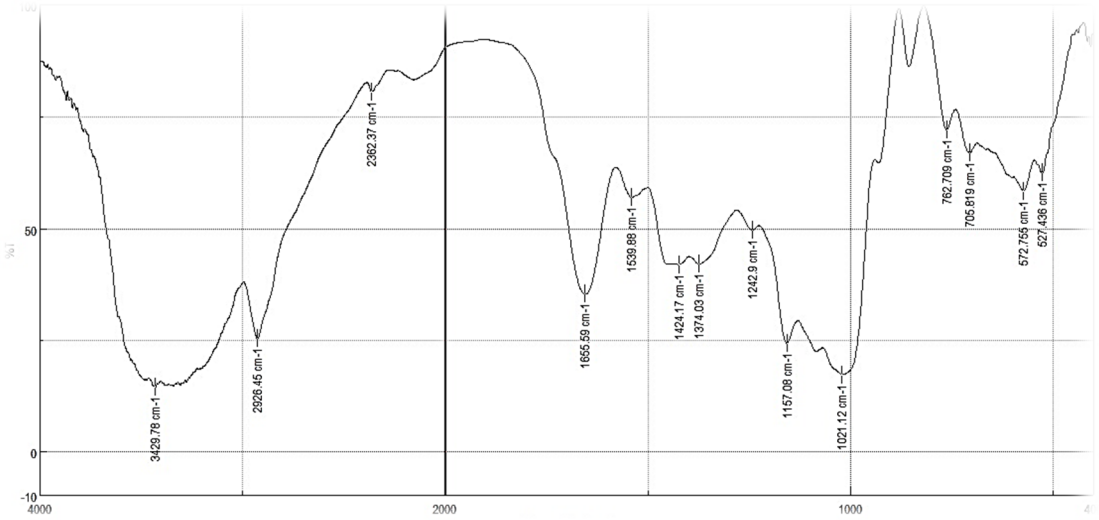

Fig. (3): FTIR analysis of *E. tef* seeds.

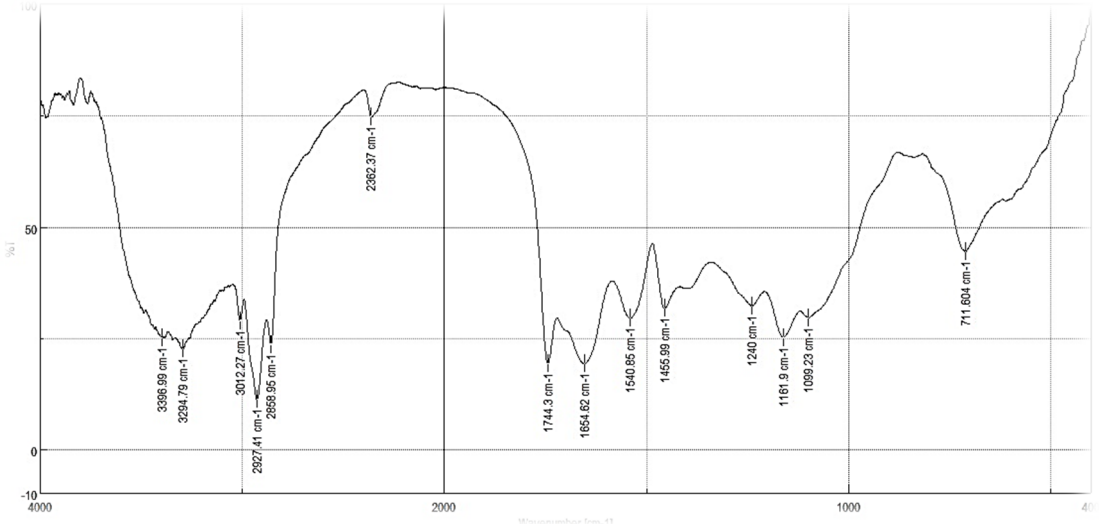

Fig. (4): FTIR analysis of *V. paradoxa* seeds.

FT-IR analysis of *V. paradoxa* seeds showed that both bands at 3396, 3294 cm^{-1} which indicate the OH stretch of the normal polymer. The range at 3012 cm^{-1} indicates the presence of the ammonium ion. Both bands 2927, 2858 cm^{-1} indicate the C-H stretch of methylene. The range at 1744 cm^{-1} indicates the presence of alkyl carbonates. The peak at 1654 cm^{-1} indicates the NH curve for the primary amine. Bar at 1540 cm^{-1} Presence of aliphatic nitro compounds. The range at 1455 cm^{-1} indicates the C-H curve of methylene. The bar at 1240 cm^{-1} indicates the aryl-O stretch of the aromatic ethers. The band at 1161 cm^{-1} indicates the CN extension of the secondary amine. The band at 1099 cm-1 is due to the C-O stretching of large rings of cyclic ethers. The bar at 711 cm^{-1} indicates the C-Cl stretch of the aliphatic chloro.

The FT-IR spectrum for both *E. tef* and *V. paradoxa* appear contain of functional groups of alkenes, aliphatic organohalogens, hydroxyl, ether, primary and secondary amines, and carbonyl compounds. The presence of the band at 2362 cm^{-1} for both *E. tef* and *V. paradoxa* is an unknown peak for both plants, and they are at the same position in the wavenumber spectrum. The FTIR results of Keshari *et al*. (2018) study confirmed

different functional groups presents on the surface of bioactive compounds. This function was responsible for capping of silver nanoparticles and stablize nanoparticles size.

The results of the study is in agreement with the study of Thirunavoukkarasu *et al.* (2013) showing FTIR spectra of aqueous silver nanoparticles prepared from *Desmodium gangeticum* leaf extract. The peaks at 3,470 cm^{-1} and 1640 cm^{-1} correspond to the N–H stretching and bending vibrations, respectively, in the amines of plant proteins. During the stretching of the OH bonds vibration at 3280 cm^{-1} (alcohol and phenol) and the CH bonds at 2,920 cm^{-1} originating from plant metabolites, the stretching of the OH-vibration at the 2,400 cm^{-1} and C=O peak at 1680 cm^{-1}, originating from a carboxylic acid. Two peaks at 1600 cm^{-1} and 1500 cm^{-1} correspond to the C = C stretching vibrations of aromatic rings, all of which are plant metabolites. Three peaks, opposite, 1010, 1190 and 1080 cm^{-1} correspond to the C-O stretch of alcohol, carboxylic acid, ester, and ether, all because of the functional groups of proteins and metabolites that cover the silver nanoparticles. The peak at 800 cm^{-1} is attributed to the aromatic groups.

Result of Philip (2010) study about green synthesis of silver nanoparticles using *Hibiscus rosa sinensis* showed that Ag nanoparticles are bound to the carboxylate ion groups from FTIR spectra. FTIR results of Dand *et al*. (2016) recorded a downward shift in the absorption bands between (800-1500 cm^{-1}) indicating the silver nanoparticles' formation using *Coffee arabica* seed extract.

Formation of AgNPs by green synthesis

Recently, green synthesis of silver nanoparticles by plants, fungi, bacteria and algae has been carried out because this is a simple, low-cost and environmentally friendly method. This technique can be a suitable alternative to physical and chemical methods.

Silver nanoparticles (AgNPs) have been widely used in industrial, household, and healthcare related products due to their excellent antimicrobial activity. With the increasing exposure of human to Ag NPs, the safety risks have attracted great interest from the public and scientists (Zhang *et al*. 2014).

As the plant extracts in this study were mixed in the aqueous solution of the silver ion compound, it began to change colour from watery to yellowish-brown to dark brown due to the silver ion reduction. Which indicate the formation of AgNPs (Figs 5 and 6).

The present study demonstrated the plant extract by reducing aqueous Ag^{+} to Ag^{0} ions, and the rapid formation of environmentally friendly silver nanoparticles with well-defined dimensions of size less than 100 nm. Although the exact mechanism of nanoparticle formation in this green synthesis is unknown, bio products or reductive cofactors apparently play a vital role in reducing salts to nanoparticles. Thus, these environmentally friendly nanoparticles can be used as an excellent source against multidrug-resistant bacteria.

This study is in agreement with the result of Thirunavoukkarasu *et al*., (2013) who concluded that the formation of silver nanoparticles was investigated by *Desmodium gangeticum* leaf extract.

The reaction was started in the first hour of incubation with silver nitrate (1m M). This was confirmed by appearance of brown in the reaction mixture. Silver nanoparticles are known to exhibit a yellowish-brown colour in aqueous solution due to excitation of surface Plasmon vibration in silver nanoparticles (Song *et al*., 2009).

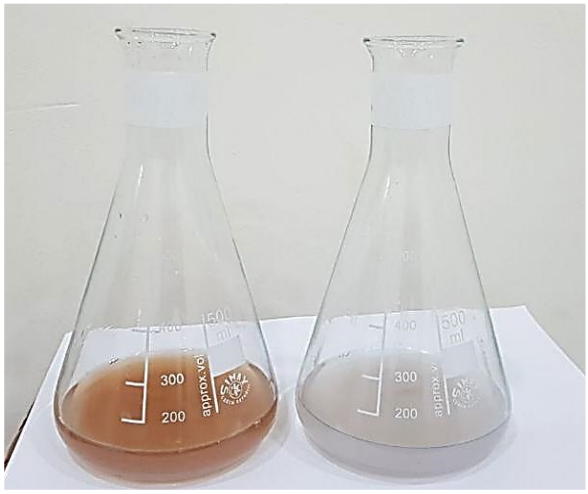

Fig. (5): AgNPs after 1 hours.

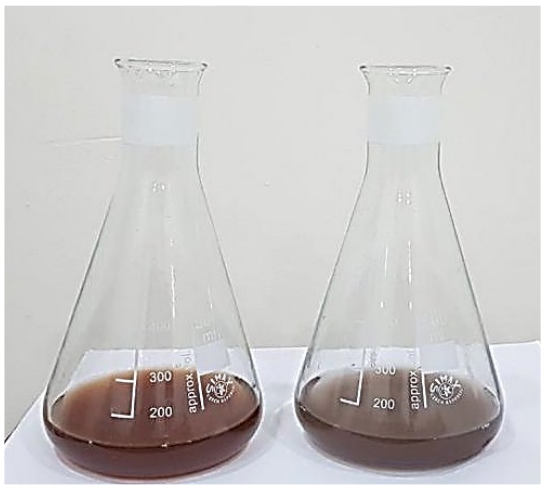

Fig. (6): AgNPs after 4 hours.

Several researchers have reported biosynthesis of nanoparticles with plant to extract for biosynthesis reaction. Plant extracts from live alfalfa, lemongrass broth, geranium leaves, and others acted as green reactive materials in the synthesis of AgNPs (Gardea-Torresday *et al*., 2003; Shankar *et al*., 2003; Shankar *et al*., 2005). Using green tea, citrus extract can be produced as reducing and stabilising agents, gold and silver nanostructures in aqueous solution under ambient conditions (Nestor *et al*., 2008). Synthesis of quasi-spherical silver nanoparticles using a purified apiin compound, extracted from the henna leaves (Kasthuri *et al*, 2009). The reaction of aqueous $AgNO_3$ with aqueous extract of leaves of common ornamental geranium plant such as *P. gravolens* produce AgNPs after 24 h. The biosynthesis of silver nanoparticles was also performed using Cycas leaf extract. The Cycas extract solution was treated with $AgNO_3$ solution and heated on the steam bath for 20 min until the colour of the solution changed to brown. The particle size ranged from 2 to 6 nm. The X-ray diffraction pattern obtained for silver nanoparticles synthesised by Cycas leaf broth show that the silver nanoparticles are crystalline (Jha & Prasad, 2010).

UV-visible Absorption Spectrum of AgNPs

It is generally recognised that UV-visible spectroscopy can be used to investigate size and shape-controlled nanoparticles in aqueous suspensions (Wiley *et al*., 2006). Figs (7 and 8) showed that the UV-Vis spectra recorded from the reaction medium after 4 h by UV spectrophotometer in the absorption range (λ 350-900 nm). The colour and absorption changes were measured at 400 nm for both *E tef* and *V. paradoxa*. The result shows that the visible light absorption ranged (from 0.20 to 0.45) for the two plant extracts. This study reported lower results than that of Thirunavoukkarasu *et al*. (2013) with are the UV-visible spectra from *Desmodium gangeticum* reaction vessel leaf extract at different times of the reaction.

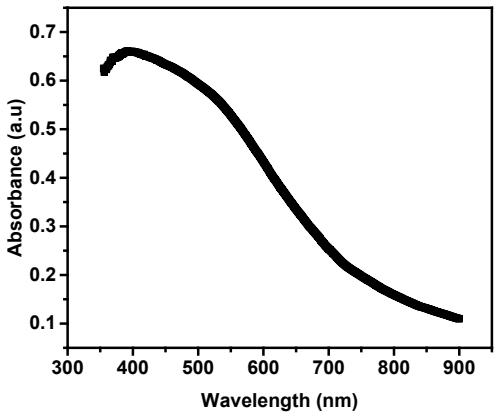

Fig. (7): UV–Vis absorption spectra for AgNPs of *E. tef*.

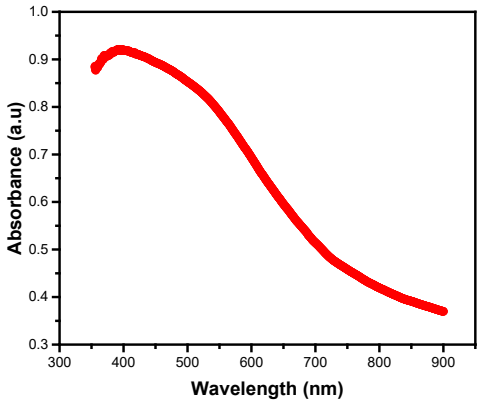

Fig. (8): UV–Vis absorption spectra for AgNPs of *V. paradoxa*.

Formation of silver nanoparticles in Keshari *et al*. (2018) study was confirmed by UV-Vis spectrophotometer (λ, 300–700 nm). The absorption band was recorded at 442 nm due to localised surface Plasmon resonance (LSPR) and confirmed the formation of silver nanoparticles. However, the lack of LSPR suggested forming of ultra-fine silver nanoparticles or the silver cluster, which contains a small number of atoms (Santos *et al*., 2015). A study of Solomon *et al*. (2013) about antimicrobial and cytotoxic effects of green synthesised silver nanoparticles using *Eucalyptus chapmaniana* leaf extract showed using UV spectroscopy that silver surface plasmon resonance band at 413 nm and this result is in agreement with the current study

The present study agree with the study by Logeswari *et al*. (2015) which showed a maximum absorption of UV-Vis spectra at 420 nm corresponding to the surface Plasmon resonance of silver nanoparticles. The observation indicated that the reduction of Ag^+ ions occurred outside the cell. It was previously reported that absorbance at around 430 nm for silver is a feature of this metal particles (Nestor *et al*., 2008).

This result is in a good agreement with the study of Khalil *et al*. (2014), the UV-Vis spectra of silver nanoparticle formation using constant $AgNO_3$ (1×10^{-3} M) concentrations at different concentrations of olive leaf extract at room temperature after 24 h. The color change of the solutions from pale yellow to yellowish-brown to dark brown depending on the concentration of the extract indicating the formation of silver nanoparticles. The change in colour was observed due to the excitation of surfactant balsamic vibration in the silver nanoparticles. It can be seen that Surface Plasmon Resonance (SPR) of Ag NPs is 440-458 nm. Kumar *et al*. (2014) conducted using extracts of the *Boerhaavia diffusa* plant as reducing agents, and UV-visible spectroscopy of a prepared silver colloidal solution showed a maximum absorption at 418 nm.

UV-visible spectroscopy result from Dhand *et al*. (2016) study showed a maximum absorption at 459 nm, representing the characteristic surface Plasmon resonance of nanoparticles using *Coffea arabica* seed extract, which agree with the current study. The UV-Vis spectrum of the study by Dadashpour *et al*. (2018) showed maximum absorption of biosynthesised AgNPs using *Matricaria chamomilla* extract at 430 nm. In the study of Saxena *et al*. (2010) about the biological synthesis of silver nanoparticles

using onion extract, the Surface Plasmon band Ag NPs solution remained close to 413 nm throughout the reaction period. In the study of Umoren *et al*. (2014), the UV-Vis absorption spectrum of the solution showed surface Plasmon resonance derived from silver nanoparticles using red apple fruit extract at ~409-448 nm. The maximum absorption peak was observed on the curve obtained for the solution containing the nanoparticles biosynthesised using aqueous extract of common sage (*Salvia officinalis*) at a wavelength of 430 nm (Zare, 2020). The result of previous study agrees well with the results from other previous studies above.

6- Scanning Electron Microscopy (SEM)

Scanning electron microscopy (SEM) analysis was performed using ESEM. Figure (9, 10) showed scanning electron micrograph of Ag NPs that mainly were spherical.

The experimental results showed that the diameter of the prepared nanoparticles in the solution was about 12.59 - 34.60 nm for AgNPs in *E. tef* seed extract and 29.05-83.94 nm in *V. paradoxa* seed extract.

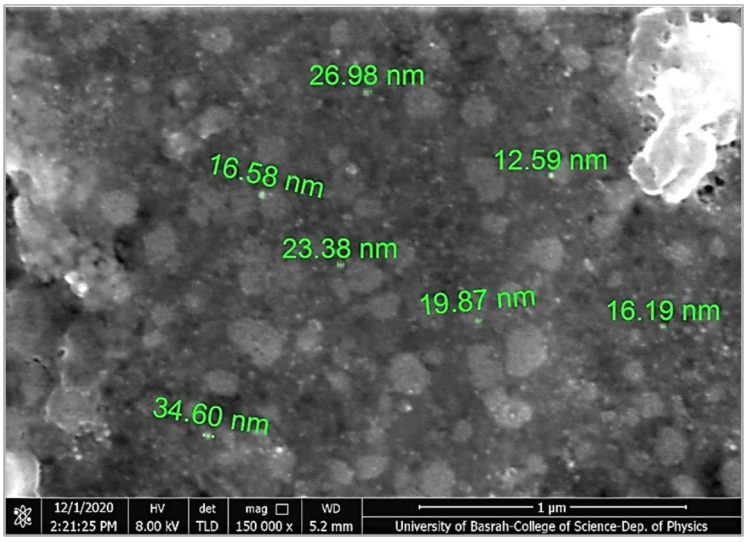

Fig. (9): SEM of AgNPs of *E. tef* seeds extracts.

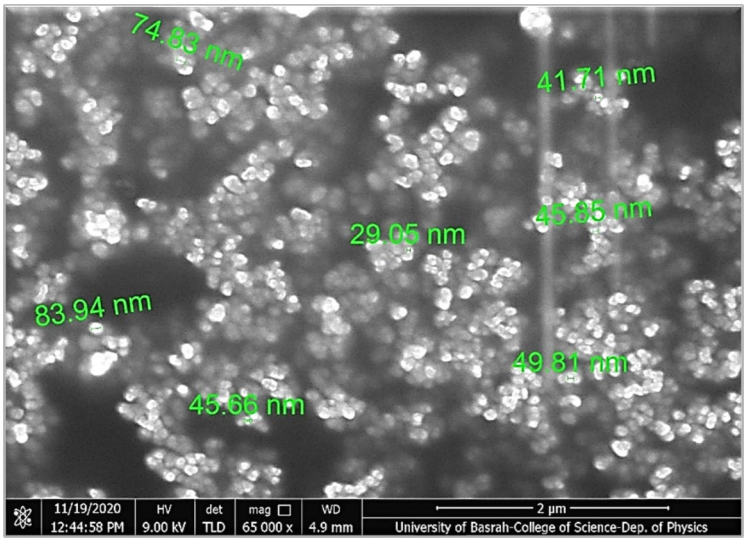

Fig.10: SEM of AgNPs of *V. paradoxa* seeds extracts

The results proved that the particles in this study are nanoparticles because their size was less than ~100 nm. The tables (8 and 9) showed there were significant differences between the two AgNPs in size below the probability level ≤ 0.05.

Table (8): Descriptive of Standard Deviation of SEM.

	N	Mean	SD	SE	Lower Bound	Upper Bound	Minimum	Maximum
A	7	21.4557	7.52339	2.84357	14.4977	28.4137	12.59	34.60
B	7	52.9786	19.36522	7.31936	35.0687	70.8884	29.05	83.94
Total	14	37.2171	21.60412	5.77394	24.7433	49.6910	12.59	83.94

Table (9): ANOVA of particle size with inhibition zone.

Sum of Squares		Df	Mean Square	F	Sig.
Between Groups	3477.917	1	3477.917	16.116	.002
Within Groups	2589.679	12	215.807		
Total	6067.595	13			

The SEM result of Keshari *et al*. (2018) confirmed that the silver nanoparticles synthesised by *Cestrum nocturnal* extract size ranged from 15 to 20 nm and they were primarily spherical which matches the results of the current study. The results of SEM analysis confirmed the presence of spherical-shaped AgNPs using the fruit extract by a vast variation in the particle size distribution with an average size of 15.5 nm by Swamy *et al*. (2015).

The dissatisfied result agree with the study of Logeswari *et al.* (2015) which concluded that the silver nanoparticle prepared using *Ocimum tenuiflorum*, *Syzygium cumini*, *Citrus sinensis*, *Solanum tricobatum*, and *Centella asiatica* respectively was 28 nm, 26.5 nm, 65 nm, 22.3 nm and 28.4 nm when the extracts were mixed with 1 m M silver nitrate solution for 24 hours. Furthermore, agreement with the result of Kumar *et al*. (2014) who showed that AgNPs preparaedin *Boerhaavia diffusa* plant extract was an average particle size of 25 nm. Moreover, the study of Saxena *et al*. (2010) concluded that AgNPs by onion extract was also in small size of 33.6 nm.

The silver nanoparticles synthesised using *Mentha piperita* plant extract were generally found to be spherical in shape with 90 nm in Mubarak Ali *et al*. (2011), which he size is larger than the resent study .Morphologically, the nanoparticles prepared by Sankar *et al*. (2013) using *Origanum vulgare* plant extract were spherical with an average particle sizedistribution of 136 ± 10.09 nm, Also Umoren *et al*. (2014) showed the average size of the synthesised silver nanoparticles using red apple fruit extract is around 150 nm. These results are bigger than the size of the current study particles, because the nanoscale size of its prepared particles exceeded 100 nm.

Diameter of inhibition zone of antibacterial activity

The antimicrobial activity of silver nanoparticles synthesised by natural plants extract was investigated against various

pathogenic organisms such as *Proteus merabilis*, *Pseudomonas aeruginosa*, *Klebsiella pneumonia*, *Acinetobacter baumannii*, and *E. coli* using well diffusion method. The diameter of inhibition zones (mm) around each well loaded with nanoparticles solution and $AgNO_3$ is represented in table (10).

Table (10): Zone of inhibition of silver nanoparticles synthesised by natural plant extracts against various pathogenic bacteria from Vitek® 2 system of hospitals (Carbapenem resistant Gram negative bacteria).

Type of Bacteria	Diameter of inhibition zone (mm)			Average	± SD
	$AgNO_3$	A*	B*		
Proteus mirabilis (ear swab)	15	20	16	17.00	2.65
Pseudomonas aeruginosa (suputum)	17	17	19	17.67	1.15
Proteus mirabilis (tissue swab)	20	21	17	19.33	2.08
Proteus mirabilis (wound swab)	20	22	18	20.00	2.00
Klebsiella pneumonia ssp. *ozaenae* (wound swab)	20	20	14	18.00	3.46
Acinetobacter baumannii complex (wound swab)	19	19	18	18.67	0.58
Pseudomonas aeroginosa (wound swab)	18	18	17	17.67	0.58
Acinetobacter baumannii (wound swab)	19	20	18	19.33	1.15
Acinetobacter baumannii (suputum)	14	15	15	14.67	0.58
Klebsiella pneumonia ssp. *pneumonia* (urine)	15	15	17	15.67	1.15
Klebsiella pneumonia ssp. *pneumonia* (wound swab)	16	13	13	14.00	1.73
Klebsiella pneumonia ssp. *pneumonia* (ear swab)	17	12	13	14.00	2.65
Acinetobacter baumannii complex (blood)	17	16	17	16.67	0.58
Acinetobacter baumannii (suputum)	18	20	18	18.67	1.15
Pseudomonas aeruginosa (blood)	16	14	14	14.67	1.15
Acinetobacter baumannii (suputum)	19	19	18	18.67	0.58
E. coli (stool)	15	20	15	16.67	2.89

A* is AgNPs using *E. tef* seeds extract; **B*** is AgNPs using *V. paradoxa* seeds extract

The result showed that the zone of bacterial inhibition by AgNPs prepared from E. tef seeds extract shows maximum inhibition at about 22mm against *Proteus mirabilis*, *Klebsiella pneumonia* ssp. *ozaenae*, and the lesser antimicrobial activity were 14mm against *Acinetobacter baumannii*. In addition silver nanoparticles synthesised by *V. paradoxa* seeds Extract were 22mm that found to be the highest antimicrobial activity against *P. mirabilis*. The lesser antimicrobial activity was 12mm against *Klebsiella pneumonia* ssp. *pneumonia*. Through the statistical analysis, no significant differences in activity were observed between the two groups of Ag NPs from plant extracts in this study versus pathological isolates as shown in tables (11 and 12). The diameter of inhibition zones (mm) around each well filled with $AgNO_3$ nanoparticles solution is represented in table (13) of the second resource of isolates from hospital sewage.

Table (11): Descriptive of inhibition zone of pathological isolates.

	N	Mean	SD	SE	Lower Bound	Upper Bound	Minimum	Maximum
A*	17	17.7059	3.01589	.73146	16.1553	19.2565	12.00	22.00
B*	17	16.2941	1.92888	.46782	15.3024	17.2859	13.00	19.00
Total	34	17.0000	2.59370	.44482	16.950	17.9050	12.00	22.00

A* is AgNPs using *E. tef* seeds extract**, B*** is AgNPs using *V. paradoxa* seeds extract

Table (12): ANOVA of inhibition zone of pathological isolates.

Sum of Squares		Df	Mean square	F	Sig.
Between Groups	16.941	1	16.941	2.644	.114
Within Groups	205.059	32	6.408		
Total	222.000	33			

Table (13): Zone of inhibition of silver nanoparticles synthesised by natural plant extracts against various ecological bacteria from hospital sewage isolates.

No. of isolate	Type of Bacteria	Diameter of inhibition zone (mm)			Average	± SD
		A*	B*	$AgNO_3$		
1	*Enterobacter cloacae* ssp. *dissolvens*	-	-	5	1.67	2.89
2	*Raoultella ornithinolytica*	7	7	7	7.00	0.00
3	*Acinetobacter baumannii*	19	18	19	18.67	0.58
4	*Acinetobacter baumannii*	17	12	15	14.67	2.52
5	*Escherichia coli*	18	14	15	15.67	2.08
6	*Escherichia coli*	15	15	15	15.00	0.00
7	*Escherichia coli*	12	-	15	9.00	7.94
8	*Enterobacter cloacae* ssp. *dissolvens*	-	-	-	0.00	0.00
9	*Enterobacter cloacae* ssp. *dissolvens*	14	6	7	9.00	4.36
10	*Enterobacter cloacae* ssp. *dissolvens*	-	-	-	0.00	0.00
11	*Enterobacter cloacae* complex	15	7	5	9.00	5.29
12	*Enterobacter aerogenes*	13	13	13	13.00	0.00
13	*Enterobacter cloacae* complex	13	13	14	13.33	0.58
14	*Enterobacter cloacae* complex	12	13	14	13.00	1.00
15	*Escherichia coli*	15	14	16	15.00	1.00
16	*Enterobacter cloacae* complex	-	-	-	0.00	0.00

*: A is AgNPs using E, tef seeds extract, B is AgNPs using V.paradox seeds extract

The result shows that there was no effect of silver nanoparticles and silver nitrate on *Enterobacter cloacae* ssp. *dissolvens*, while there was a clear effect on *Acinetobacter baumannii.* The result of the statistical analysis, no significant differences in activity were observed between the two groups of AgNPs from plant extracts in this study versus pathological isolates shown in tables (14 and 15).

Table (14): Descriptive of inhibition zone of ecological isolates.

N		Mean	SD	SE	Lower Bound	Upper Bound	Minimum	Maximum
A*	16	10.6250	6.89807	1.72452	6.9493	14.3007	.00	19.00
B*	16	8.2500	6.51665	1.62916	4.7775	11.7225	.00	18.00
Total	32	9.4375	6.71031	1.18623	7.0182	11.8568	.00	19.00

A* is AgNPs using *E. tef* seeds extract, **B*** is AgNPs using *V. paradoxa* seeds extract

Table (15): ANOVA of inhibition zone of ecological isolates.

Sum of Squares		Df	Mean square	F	Sig.
Between Groups	45.125	1	45.125	1.002	.325
Within Groups	1350.750	30	45.025		
Total	1395.875	31			

The results of current study corresponds with Logeswari *et al*. (2015), it was found that silver nanoparticles synthesised by *Solanum tricobatum*, *Ocimum tenuiflorum* extracts showed highest antimicrobial activity against *E. coli* (30 mm) and lesser activity of silver nanoparticles synthesised by *Tricobacterium solanum* extract was against *P. aeruginosa* (12 mm) and *E. coli* (12 mm). Studies of (Sondi & Salopek-Sondi, 2004; Morones *et al*., 2005) concluded that silver nanoparticles exhibited effective antimicrobial properties compared to other salts due to their extensive surface area, better contact with microorganisms. The nanoparticles get attached to the cell membrane, then penetrated inside the bacteria. The bacterial membrane contains sulfur-containing proteins and silver nanoparticles interact with these proteins and the phosphorous-containing compounds such as DNA. When the nanoparticles enter the bacterial cell, it forms a low molecular weight region in the center of the bacteria to which the bacteria conglomerates, thus protecting the silver ions' DNA. Preferably, nanoparticles attack the respiratory chain and cell division eventually leads to cell death. Silver nanoparticles biosynthesised using *Origanum vulgare* extract were found to be impressive in inhibiting human pathogens (*Escherichia coli* inhibition area 12 mm, and *Klebsiella* ssp. 9 mm) (Sankar *et al*., 2013).

Anticancer activity

The results showed that the nanomaterials in this study have a common toxic effect on normal cells and this is what it is observed in the drugs used in the treatment of cancer as they have many side effects.

1- Cancer cell line

A: AgNPs using seeds of *Eragrostis tef*

Table (16): Rate viability of mcf7 cell line treated with three replicate of concentrations (µg.ml^{-1})

Concentration of materials%	AgNPs (50)	AgNPs (75)	Extract(50)	Ag NO_3 (50)	Mean	±SD
Mean of viability %	27.09	22.88	72.98	29.85	38.20	23.36
Mean of toxicity %	72.91	77.12	27.02	70.15	61.80	23.36

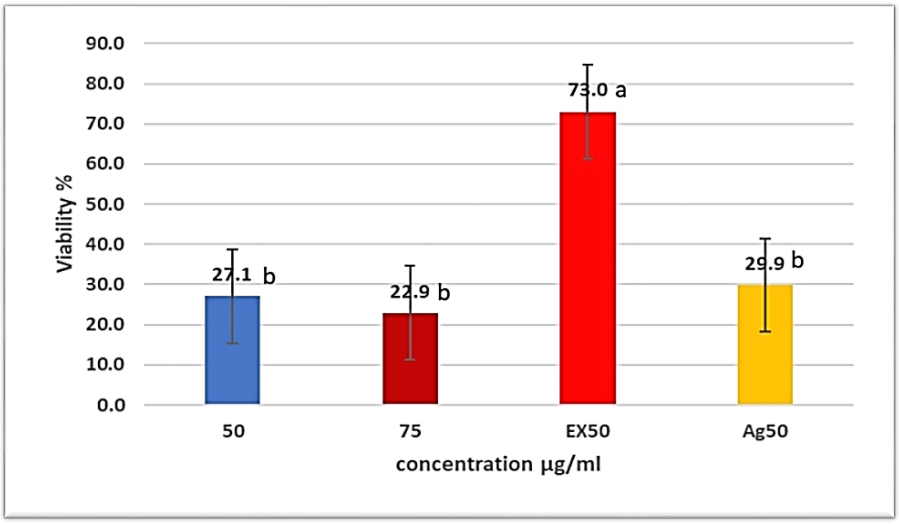

Fig. (11): Rate viability of mcf7 cell line treated with three replicate of concentrations (µg.ml^{-1})

B: AgNPs using seeds of *Vitellaria paradoxa*

Table (17): Rate viability of mcf7 cell line treated with three replicate of concentrations (µg.ml^{-1})

Concentration of materials%	AgNPs (50)	AgNPs (75)	Extract (50)	Ag NO_3 (50)	Mean	±SD
Mean of viability %	22.77	23.77	20.23	29.85	24.16	4.08
Mean of toxicity %	77.23	76.23	79.77	70.15	75.85	4.08

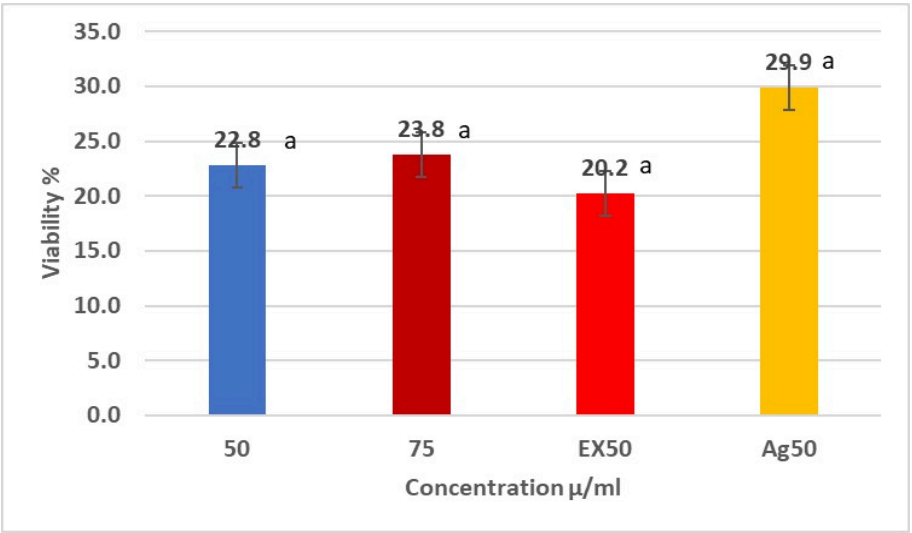

Fig. (12): Rate viability of mcf7 cell line treated with three replicate of concentrations (µg.ml^{-1})

2- Normal cell line

A: AgNPs using seeds of *Eragrostis tef*

Table (18): Rate viability of HBL100 cell line treated with three replicate of concentrations (µg.ml^{-1})

Concentration of materials%	AgNPs (50)	AgNPs (75)	Extract 50	Ag NO_3 (50)	Mean	±SD
Mean of viability %	41.53	42.25	74.67	53.54	53.00	15.46
Mean of toxicity %	58.47	57.75	25.33	46.46	47.00	15.46

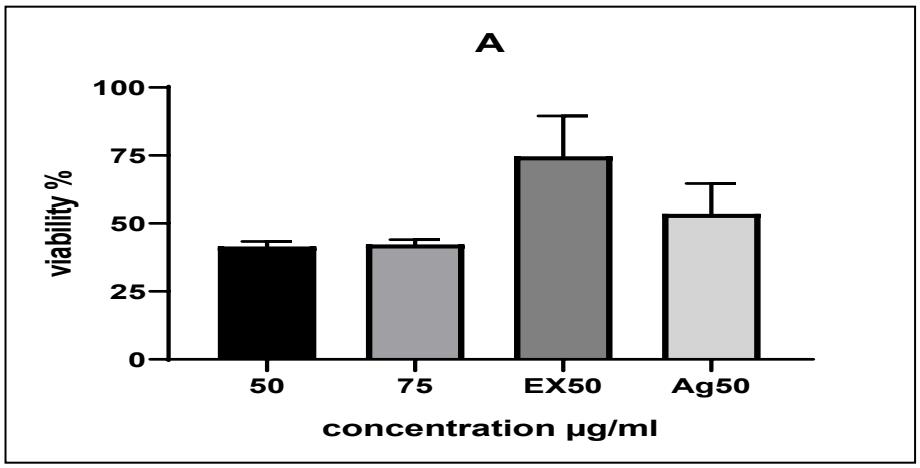

Fig. (13): Rate viability of HBL100 cell line treated with three replicate of concentrations (µg.ml^{-1})

B: AgNPs using seeds of *Vitellaria paradoxa*

Table (19): Rate viability of HBL100 cell line treated with three replicate of concentrations (µg.ml^{-1})

Concentration of materials%	AgNPs (50)	AgNPs (75)	Extract (50)	Ag NO_3 (50)	Mean	SD
Mean of viability %	58.58	56.90	39.13	53.54	52.04	8.86
Mean of toxicity %	41.42	43.10	60.87	46.46	47.96	8.86

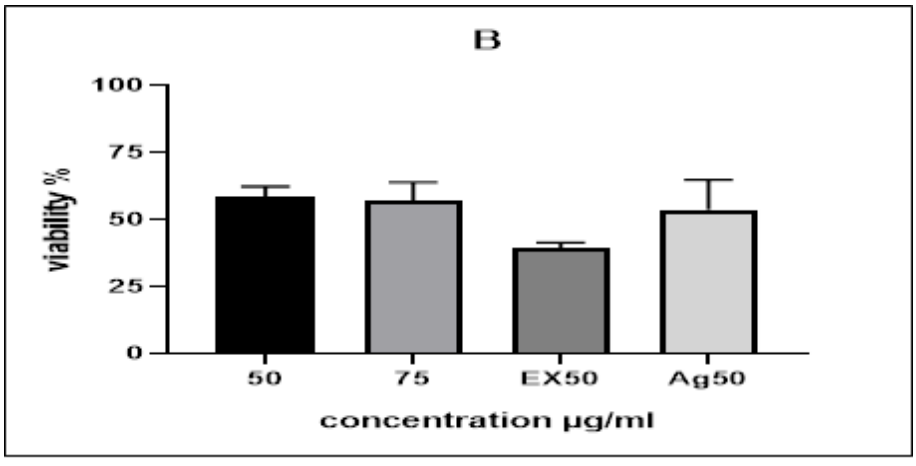

Fig. (14): Rate viability of HBL100 cell line treated with three replicates of concentrations (µg.ml^{-1}).

The synthesis of silver nanoparticles significantly inhibited many pathogenic organisms and reduced the viability of HL-60 cells in a dose-dependent manner from Sulaiman *et al*. (2013) study on silver nanoparticles using eucalyptus leaf extract.

In vitro cytotoxicity of AgNPs using *Matricaria chamomilla* plant extract in Dadashpour *et al*., (2018) showed a dose-and time-dependent cytotoxic effect against A549 lung cancer cells. Green silver nanoparticles synthesized using *Origanum vulgare* extract showed a dependent response to human lung cancer A549 cell line (LD_{50}-100 $\mu g.ml^{-1}$) (Sankar *et al*., 2013).

Result of Swamy *et al*. (2015) study about AgNPs using *Momordica cymbalaria* fruit extract showed the cytotoxicity towards Rat L6 skeletal muscle cell line at different concentration, but the highest inhibition percentage was recorded for Ag NPs at a concentration 100% $mcg.ml^{-1}$.

AgNPs exhibited a killing rate of 40% in MCF-7 cells (the cancer cell model) at a concentration of 100 µg/ml with almost no effect on Vero cells (the normal cell model). (Sangour *et al*., 2021).

The Results of (Al-Ali & Jawad, 2021) study revealed that there is cytotoxicity of the two substances CeO_2NP and Retinoic acid (RA) on the cell lines (MCF-7, CaL51, & HBL-100) and that the levels of vitality decrease with increasing concentration, except for the normal cell line HBL-100, that their vitality increases with the increase in the concentration of the substance.

Conclusions

Nature has elegant and innovative ways to create the most efficient miniaturised functional materials. Increasing awareness of green chemistry and using the green route to synthesise metal nanoparticles lead to a desire to develop environmentally friendly technologies. The benefit of synthesizing silver nanoparticles using plant extracts is an economical, energy efficient and cost effective method. Hence, this is the first time that these plant extracts have been used as antibacterial and anticancer action. Therefore, the use of plant seed extracts (of *E. tef* and *V. paradoxa*) for the green synthesis of silver nanoparticles could constitute a tremendous impact in the coming decades.

Acknowledgements

We would like to thank and gratitude Dr. Ali A. A. Al-Ali, Department of Biology, College of Pure Sciences, University of Basrah for his assistance in anticancer activity test; to Dr. Abdullah A. Hussein, Director of the Polymer Center, for his help in handling different experiments and to Dr. Emad Y. Awad, Department of Biology, College of Pure Sciences for his help in the statistical analysis.

Contributions of Authors

S.M.A.M.S: Sample collection, data collection, Laboratory methodology, and write the manuscript.

M.A.A.Q.A: Suggest a title of the research, Read and revise the manuscript.

References

Adekunle, A. S., & Adekunle, O. C. (2009). Preliminary assessment of antimicrobial properties of aqueous extract of plants against infectious diseases. *Biology and Medicine 1*(3), 20-24. https://www.cabdirect.org/cabdirect/abstract/20103234843

Ahmed, A., Mukherjee, P., Senapati, S., Mandal, D., Khan, MI., Kumar, R., & Sastry, M. (2003). Extracellular biosynthesis of silver nanoparticles using the fungus *Fusarium oxysporum*. *Colloids Surf B: Biointerfaces, 28*, 313-318. https://doi.org/10.1016/S0927-7765 (02)00174-1

Ahmed, Sh., Ahmad, M., Swami B. L., & Ikram S. (2016). A review on plants extract mediated synthesis of silver nanoparticles for antimicrobial applications: A green expertise. *Journal of Advanced Research, 7*(1), 17-28. https://doi.org/10.1016/j.jare.2015.02.007

Al-Ali, A. A., & Jawad, R. K. (2021). Cerium oxide nanoparticles Ceo2np and retinoic acid trigger cytotoxicity and apoptosis pathway in human breast Cell Lines. *Annals of the Romanian Society for Cell Biology*, *25*(4), 8448-8477.

Al-Hamdani M. A., & Abas I. J. (2013). Study of plasmid profile and susceptibility patterns of *Escherichia coli* isolated from patients with urinary tract infection in Basra. *Journal of Thi-Qar Sciences*, *4*(1), 31-39.

Al-Hamdani M, Akbar M. M, Saed S. M. (2020). Seasonal Variation, Antibiotic Resistance of Some Sewage Bacteria from Hamdan Waste Water Treatment Plant in Basrah City-Iraq. *Journal of Global Pharma Technology*, *12*(2), 147-153.

Al-Marjani, F. M., Makarim, A. K., Jabari, Z. H., & Zaid, N. H. (2010). Detection of multidrug resistant *Pseudomonas aeroginosa* isolates producing IMP-1 Metallo-β-Lactamase in some Baghdad hospitals. *Tikrit Journal of Pure Science, 15*(1), 188-192.

Al-Musawi Z. & Al-Saadi N. (2021). Antitumor activities of biosynthesized silver nanoparticles using *Dodonaea viscosa* (L.) leaves extract. *Basrah Journal of Agricultural Sciences, 34*(2), 42-59. https://doi.org/10.37077/25200860.2021.34.2.04

Al-Rubaye, A. F., Hameed, I. H., & Kadhim, M. J. (2017). A review: Uses of gas chromatography-mass spectrometry (GC-MS) technique for analysis of bioactive natural compounds of some plants. *International Journal of Toxicological and Pharmacological Research*, *9*(1), 81-85. https://doi.org/10.25258/ijtpr.v9i01.9042

Al-Shammari, A. M., Alshami, M. A., Umran, M. A., Almukhtar, A. A.; Yaseen, N. Y., Raad, K., & Hussien, A. A. (2015). Establishment and characterisation of a receptor-negative, hormone-nonresponsive breast cancer cell line from an Iraqi patient. *Breast Cancer: Targets Ther, 7,* 223-230. https://doi.org/10.2147/BCTT.S74509

Al-Shammari, A. M., Al-Esmaeel, W. N., Al-Ali, A. A., Hassan, A. N. A., & Ahmed, A. A. (2019). Enhancement of oncolytic activity of Newcastle disease virus through combination with retinoic acid against digestive system malignancies. *Molecular Therapy, 27*(4S1), 126-127.

Anandalakshmi, K., Venugobal, J., & Ramasamy, V. (2016). Characterisation of silver nanoparticles by green synthesis method using Pedalium murex leaf extract and their antibacterial activity. *Applied Nanoscience, 6*, 399-408. https://link.springer.com/article/10.1007/s13204-015-0449-z

Animasaun, D. A, Oyedeji, S, Olorunmaiye, K. S, Azeez, M. A., Tijani, I. A., & Morakinyo, J. A. (2019). Morpho-chemical divergence and fatty acid profile of shea tree seeds (*Vitellaria paradoxa*) collected from different locations in Kwara State, Nigeria. *Acta Botanica Croatica, 78*(1), 17-24. https://doi.org/10.2478/botcro-2019-0002

Anoar, A. K., Ali, F. A., & Sherko, A. O. (2014). Detection of metallo β-lactamase enzyme in some gram negative bacteria isolated from burn patients in Sulaimani city, Iraq. *European Scientific Journal, 10*(3), 1875-1887.

Balaj, K., Kilimozhi, D., & Parthasarathy, V. (2014). GC-MS analysis of various extracts of *Clerodendrum phlomidis* leaf. *International Journal of Pharmacy and Pharmaceutical Sciences, 6*(1), 226-232.

Bharathy, V., Maria Sumathy, B., & Uthayakumari, F. (2012). Determination of phytocomponents by GC-MS in leaves of *Jatropha gossypifolia*. *Science Research Reporter. 2*(3), 286-290.

Bodoprost, H., & Rosemeyer, J. (2007). Analysis of phenacylester derivatives of fatty acids from, Human skin surface Sebum by RP-HPLC: Chromatograpic mobility as a function of physiochemical properties. *International Journal of molecular Sciences*, *8*(11), 1111-1124. https://doi.org/10.3390/i8111111

Boka, B., Woldegiorgis, A. Z, & Haki, G. D. (2013). Antioxidant properties of Ethiopian traditional bread (*injera*) as affected by processing techniques and tef grain (*Eragrostis tef* (Zucc.)) varities. *Canadian Chemical Transactions*, *1*(2), 7-24. http://doi.org/10.13179/canchemtrans.2013.01.01.0012

Dadashpour, M., Firouzi-Amandi, A., Pourhassan-Moghaddam, M., Maleki, M. J., Soozangar, N.,

Jeddi, F., Nouri, M., Zarghami, N., & Pilehvar-Soltanahmadi, Y. (2018). Biomimetic synthesis of silver nanoparticles using *Matricaria chamomilla* extract and their potential anticancer activity against human lung cancer cells. *Materials Science and Engineering: C, 92*, 902-912. https://doi.org/10.1016/j.msec.2018.07.053

Dhand, V., Soumya, L., Bharadwaj, S., Chakra, Sh., Bhatt, D., & Sreedhar, B. (2016). Green synthesis of silver nanoparticles using *Coffea arabica* seed extract and its antibacterial activity. *Materials Science and Engineering: C, 58*, 36-43. https://doi.org/10.1016/j.msec.2015.08.018

Datta, P., Gupta, V., Garg, S., & Chander, J. (2012). Phenotypic method for differentiation of carbapenemase in *Enterobacteriaceae*: study from north India. *Indian Journal Pathology Microbiology, 55*(3), 357-360. https://doi.org/10.4103/0377-4929.101744

Esterly, J. S., Wagner, J., McLaughlin, M. M., Postelnick, M. J., Qi, C., & Scheetz, M. H. (2012). Evaluation of clinical outcomes in patients with bloodstream infections due to gram-negative bacteria according to carbapenem MIC stratification. *Antimicrobial Agents Chemotherapy 56*, 4885-4890. http://doi.org/10.1128/AAC.06365-11

Feliciano, A., Medarde, M., Del Rey, B., Del Corral, J., & Barrero, A. (1990). Eudesmane glycosides from *Carthamus lanatus*. *Phytochemistry, 29*, 3207-3211. https://doi.org/10.1016/0031-9422 (90)80186-K

Freshney, R. I. (2010). *Culture of animal cells a manual of basic technique and specialized applications*. Sixth edition, Wiley-Blackwell, 732pp. https://doi.org/10.1002/9780470649367

Gardea-Torresdey J. L., Gomez, E., Videa, J. R. P., Troiani, H., & Yacaman, M. J. (2003). Alfalfa sprouts: a natural source for the synthesis of silver nanoparticles. *Langmuir, 19*, 1357-1361. https://doi.org/10.1021/la020835i

Grover, N., & Patni, V. (2013). Phytochemical characterization using various solvent extracts and GC-MS analysis of methanolic extract of woodfordia fruticosa leaves. *International Journal of Pharmacy and Pharmaceutical Sciences*, *5*, 291-295.

Guh, A. Y., Limbago, B. M., & Kallen, A. J. (2014). Epidemiology and prevention of carbapenem-resistant *Enterobacteriaceae* in the United States. *Expert Review of Anti-infective Therapy, 12*(5), 565-580. http://doi.org/10.1586/14787210.2014.902306

Gupta, E., Mohanty, S., Sood, S., Dhawan, B., & Das, B. K. (2006). Emerging resistance to carbapenems in a tertiary care hospitalin north India. *The Indian Journal of Medical Research*, *124*(1): 95-98.

Gupta, N., Limbago, B. M., Patel, J. B., & Kallen, A. J. (2011). Carbapenem-resistant Enterobacteriaceae: epidemiology and prevention. *Clinical Infectious Diseases 53*, 60-67. http://doi.org/10.1093/cid/cir202.

Jha, K. A. & Prasad, K. (2010). Green synthesis of silver nanoparticles using Cycas leaf. *International Journal of Green Nanotechnology: Physics and Chemistry, 1*(2), 110-117. https://doi.org/10.1080/19430871003684572

Kala, S. M. J., Balasubramanian, T., Tresina Soris, S., & Mohan, V. R. (2011). GC-MS determination of bioactive components of *Eugenia singampattiana* Bedd. *International Journal of ChemTech Research, 3*, 1534-1537.

Kasthuri, J., Veerapandian, S., & Rajendiran, N. (2009). Biological synthesis of silver and gold nanoparticles using apiin as reducing agents. *Colloids and Surfaces B: Biointerfaces, 68*, 55-60. https://doi.org/10.1016/j.colsurfb.2008.09.021

Kaviya, S. S. J., & Viswanathan, B. (2011). Green synthesis of silver nanoparticles using *Polyalthia longifolia* leaf extract along with D-sorbitol. *Journal of Nanotechnology*, *2011*, Article ID 152970, 1-5. https://doi.org/10.1155/2011/152970

Keshari, A. K., Srivastava, R., Singh, P., Yadav, V. B., & Nath, G. (2018). Antioxidant and antibacterial activity of silver nanoparticles synthesised by *Cestrum nocturnum. Journal of Ayurveda and Integrative Medicine, 11*, 37-43. https://doi.org/10.1016/j.jaim.2017.11.003

Khalil, K. A., Fouad, H., Elsarnagawy, T., & Almajhdi, F. N. (2013). Preparation and characterisation of electrospun PLGA/silver composite nanofibers for biomedical applications. *International Journal of Electrochemical Science*, *8*, 3483-3493.

Khalil, M. M. H, Ismail, E. H., El-Baghdady, K. Z., & Mohamed, D. (2014). Green synthesis of silver nanoparticles using olive leaf extract and its antibacterial activity. *Arabian Journal of Chemistry, 7*(6), 1131-1139. https://doi.org/10.1016/j.arabjc.2013.04.007

Klaus-Joerger, T., Joerger, R., Olsson, E., & Granqvist, C. (2001). Bacteria as workers in the living factory: metal accumulating bacteria and their potential for materials science. *Trends in Biotechnology, 19*, 15-20. https://pubmed.ncbi.nlm.nih.gov/23318667/

Korbekandi, H. & Iravani, S. (2012). Chapter: 1, *Silver nanoparticles, the delivery of nanoparticles.* 1-36. In Hashim, A. A. (Ed.). *Advances in Nanocomposite Technology*. IntechOpen. 388pp. https://doi.org/10.5772/34157

Kumar, P. P., Kumaravel, S., & Lalitha, C. (2010). Screening of antioxidant activity, total phenolics and GC-MS study of *Vitex negundo*. *African Journal Biochemistry Research, 4*(7), 191-195. https://doi.org/10.5897/AJBR.9000213

Kumar, P.P., Pammi, S.V., Kollu, P., Satyanayarana, K., & Shameem, U. (2014). Green synthesis and characterisation of silver nanoparticles using Boerhaavia diffusa plant extract and their anti-bacterial activity. *Industrial Crops and Products, 52,* 562-566. https://doi.org/10.1016/j.indcrop.2013.10.050

Lewis, K., & Ausubel, F. M. (2006). Prospects for plant-derived antibacterials. *Nature Biotechnology*, *24*(12), 1504-1507. https://doi.org/10.1038/nbt1206-1504

Logeswari, P., Silambarasan**, S**., & Abraham, J. (2015). Synthesis of silver nanoparticles using plants extract and analysis of their antimicrobial property. *Journal of Saudi Chemical Society, 19*(3), 311-317. https://doi.org/10.1016/j.jscs.2012.04.007

Lu, Z., Rong, K., Li, J., Yang, H., & Chen, R. (2013). Size-dependent antibacterial activities of silver nanoparticles against oral anaerobic pathogenic bacteria. *Journal of Materials Science Material Medicine*, *24*(6), 1465-1471. https://doi.org/10.1007/s10856-013-4894-5

Manoharan, A., Premalatha, K., Chatterjee, S., & Mathai, D. (2011). Correlation of TEM, SHV, and CTx-M extended-spectrum beta lactamase among *Enterobacteriaceae* within their in vitroantimicrobial susceptibility. *Indian. Journal of Medical Microbiology, 29*(2), 161-164. https://doi.org/10.4103/0255-0857.81799

Mittal, A.K., Chisti, Y., & Banerjee, U. C. (2013). Synthesis of metallic nanoparticles using plant extracts. *Biotechnology Advances, 31*(2), 346-356. https://doi.org/10.1016/j.biotechadv.2013.01.003

Morones, J. R., Elechiguerra, J. L., Camacho, A., Holt, K., Kouri, J. B, Ramirez, J. T., & Yacaman, M. J. (2005). The bactericidal effect of silver nanoparticles. *Nanotechnology, 16,* 2346-2353 https://doi.org/10.1088/0957-4484/16/10/059

Mubarak Ali, D., Thajuddin, N., Jeganathan, K., & Gunasekaran, M. (2011**).** Plant extract mediated synthesis of silver and gold nanoparticles and its antibacterial activity against clinically isolated pathogens. *Colloids and Surfaces B: Biointerfaces, 85*(2), 360-365. https://doi.org/10.1016/j.colsurfb.2011.03.009

Nestor, A. R. V., Mendieta, V. S., Lopez, M. A. C., Espinosa, R. M. G., Lopez, M. A. C., & Alatorre, J. A. A. (2008). Solventless synthesis and optical properties of Au and Ag nanoparticles using *Camiellia sinensis* extract. *Materials Letters*, *62*(17-18), 3103-3105. https://doi.org/10.1016/j.matlet.2008.01.138

Pal, S., Tak, Y. K., & Song, J. M. (2007). Does the antibacterial activity of silver nanoparticles depend on the shape of the nanoparticle? A study of the Gram-negative bacterium *Escherichia coli*. *Applied and Environmental Microbiology*, *73*(6), 1712-1720. http://doi.org/10.1128/AEM.02218-06

Philip, D. (2010). Green synthesis of gold and silver nanoparticles using *Hibiscus rosa sinensis*. *Physica E: Low-dimensional Systems and Nanostructures*, *42*(5), 1417-1424. https://doi.org/10.1016/j.physe.2009.11.081

Prabhu, S., & Poulose, E. K. (2012). Silver nanoparticles: mechanism of antimicrobial action, synthesis, medical applications, and toxicity effects. *International Nano Letters*, *2*(1), 1-42. https://doi.org/10.1186/2228-5326-2-32

Sangour, M. H., Ali, I. M., Atwan, Z. W., & Al-Ali A. A. (2021). Effect of Ag nanoparticles on viability of MCF-7 and Vero cell lines and gene expression of apoptotic genes. *Egyptian Journal of Medical*

Human Genetics, 22(9). https://doi.org/10.1186/s43042-020-00120-1

Sankar, R., Karthik, A., Prabu, A., Karthik, S., Shivashangari, K. S., & Ravikumar, V. (2013). *Origanum vulgare* mediated biosynthesis of silver nanoparticles for its antibacterial and anticancer activity. *Colloids and surfaces. B, Biointerfaces, 108,* 80-84. https://doi.org/10.1016/j.colsurfb.2013.02.033

Santhosh, K. S., Samydurai, P., Ramakrishnan, R., & Nagarajan, N. (2014). Gas chromatography and mass spectrometry analysis of bioactive constituents of *Adiantum capillus-veneris* L. *International Journal of Pharmaceutical Sciences*, *6*(4), 60-63.

Santos, E. D. B., Madalossi, N. V., Sigoli, F. A., & Mazali, I. O. (2015). Silver nanoparticles: green synthesis, self-assembled nanostructures and their application as SERS substrates. *New Journal of Chemistry*, *39*, 2839-2846. https://doi.org/10.1039/C4NJ02239D

Sarac, N., & Ugur, A. (2009). The *in vitro* antimicrobial activities of the essential oils of some Lamiaceae species from Turkey. *Journal of Medicinal Food*, *12*, 902-907. https://doi.org/10.1089/jmf.2008.0089

Satyavani, K., Ramanathan, T., & Gurudeeban, S. (2011). Green synthesis of silver nanoparticles by using stem derived callus extract of bitter apple (*Citrullus colocynthis*). *Digest Journal of Nanomaterials and Biostructures, 6*(3), 1019-1024. https://doi.org/10.3923/ajbkr.2011.246.253

Saxena, A., Tripathi, R. M., & Singh, R. P. P. (2010). Biological synthesis of silver nanoparticles by using onion (*Allium cepa*) extract and their antibacterial activity. *Digest Journal of Nanomaterials and Biostructures, 5*, 2, 427-432.

Shankar, S., Ahmed, A., & Sastry, M. (2003). Geranium leaf assisted biosynthesis of silver nanoparticles. *Biotechnology Program*, *19,* 1627-1631. https://doi.org/10.1021/bp034070w

Shankar, S., Rai, A., Ahmed, A., & Sastry, M. (2005). Controlling the optical properties of lemongrass extract synthesised gold nanotriangles and potential application in infrared-absorbing optical coatings. *Chemistry Materials*, *17,* 566-572. https://doi.org/10.1021/cm048292g

Singh, A., Jain, D., Upadhyay, M. K., Khandelwal, N., & Verma, H. N. (2010). Green synthesis of silver nanoparticles using *Argemone mexicana* leaf extract and evaluation of their antimicrobial activities. *Digest Journal of Nanomaterials and Biostructures*. *5*(2), 483-489.

Slayton, R. B., Toth, D., Lee, B.Y., Tanner, W., Bartsch, S. M., Khader, K., Wong, K., McKinnell, J. A., Ray, W., Miller, L. G., Rubin, M., Kim, D. S., Adler, F., Cao, C., Avery, L., Stone, N. T. B., Kallen, A., Samore, M., Huang, S. S., Fridkin, S., & Jernigan, J. A. (2015). Vital signs: estimated effects of a coordinated approach for action to reduce antibiotic-resistant infections in health care facilities-United States. *(MMWR) Morbidity and Mortality Weekly Report*, *64*, 826-831. http://doi.org/10.15585/mmwr.mm6430a4

Sondi, I., & Salopek-Sondi, B. (2004). Silver nanoparticles as antimicrobial agents: a case study on *E. coli* as a model for Gram-negative bacteria. *Journal of Colloids and Interface Science*, *275*, 177-182. https://doi.org/10.1016/j.jcis.2004.02.012

Song, J. Y., Kwon, E. -Y., & Kim, B. S. (2009). Biological synthesis of platinum nanoparticles using *Diopyros kaki* leaf extract. *Bioprocess and Biosystems Engineering*, *32*, 79-84. https://doi.org/10.1007/s00449-009-0373-2

Sulaiman, G., Mohammed, W., Marzoog, T, Al-Amiery, A., Kadhum, A., & Mohamad, A. (2013). Green synthesis, antimicrobial and cytotoxic effects of silver nanoparticles using *Eucalyptus chapmaniana* leaves extract. *Asian Pacific Journal of Tropical Biomedicine, 3*(1), 58-63. https://doi.org/10.1016/S2221-1691 (13)60024-6

Swamy, M. K., Akhtar, M. S., Mohanty, S. K., & Sinniah, U. R. (2015). Synthesis and characterisation of silver nanoparticles using fruit extract of *Momordica cymbalaria* and assessment of their *in vitro* antimicrobial, antioxidant and cytotoxicity activities. *Spectrochimica Acta Part A: Molecular and Biomolecular Spectroscopy, 151*, 939-941. https://doi.org/10.1016/j.saa.2015.07.009

Thirunavoukkarasu, M., Balaji, U., Behera, S., Panda, P. K., & Mishra, B. K. (2013). Biosynthesis of silver nanoparticles from leaf extract of *Desmodium gangeticum* (L.) DC. and its biomedical potential. *Spectrochimica Acta Part A: Molecular and*

Biomolecular Spectroscopy, 116, 424-427. https://doi.org/10.1016/j.saa.2013.07.033

Umoren, S. A., Obot, I. B., & Gasem, Z. M. (2014). Green synthesis and characterisation of silver nanoparticles using red apple (*Malus domestica*) fruit extract at room temperature. *Journal of Materials and Environmental Science, 5*, 3, 907-914.

Vasoo, Sh., Barreto, J. N., & Tosh, P. K. (2015). Emerging issues in gram-negative bacterial resistance: an update for the practicing clinician. *Mayo Clinic Proceedings*, *90*, 395-403. http://doi.org/10.1016/j.mayocp.2014.12.002

Wiley, B., Im, S., Li, Z., McLellan, J., Siekkinen, A., & Xia, Y.(2006). Maneuvering the Surface Plasmon Resonance of Silver Nanostructures through Shape-Controlled Synthesis. *Journal of Physical Chemistry B, 110*, 32, 15666-15675. https://doi.org/10.1021/jp0608628

Zare, H. (2020). Biosynthesis of silver nanoparticles using common sage extract and evaluation of the anticancer activity. *Biomedical Journal of Scientific & Technical Research, 28*, 1, 21179-21185. https://doi.org/10.26717/BJSTR.2020.28.004581

Zhang, T., Wang, L., Chen, Q., & Chen, Ch. (2014). Cytotoxic potential of silver nanoparticles. *Yonsei Medical Journal, 55*, 2, 283-291. https://doi.org/10.3349/ymj.2014.55.2.283

التأثيرات المضادة للبكتيريا والسرطان لجزيئات الفضة النانوية المصنعة باستخدام مستخلص بذور نبات التيف *Eragrostis tef* وبذور نبات الشياه *Vitellaria paradoxa*

سهى محمد علي محمد سعيد المظفر وميثم أيوب عبد القادر الحمداني

قسم علوم الحياة، كلية العلوم الصرفة، جامعة البصرة، العراق

المستخلص: تهدف الدراسة الحالية إلى التحقيق في التخليق الحيوي لجسيمات الفضة النانوية باستخدام المستخلص المائي لبذور نبات *Eragrostis tef* (نبات التيف أو الحشيش السنوي) ومستخلص بذور *Vitellaria paradoxa* (شجرة زبدة الشيا) والتحقيق في أنشطتها المضادة للميكروبات والسرطان. من أجل تصنيع الجسيمات النانوية الفضية ، تم تحضير المستخلص المائي للنبات وإدخاله في محلول نترات الفضة 1 ملي مولار. تم تمييز Ag NPs المُصنَّع باستخدام تقنيات مفيدة مختلفة بما في ذلك التحليل الطيفي المرئي فوق البنفسجي (UV–Vis)، والتحليل الطيفي للأشعة تحت الحمراء (FTIR)، والميكروسكوب الإلكتروني (SEM). لوحظ رنين البلازمون السطحي (SPR) لـ Ag NPs باستخدام مستخلص بذور *E.tef* و *V. paradoxa* عند 40 نانومتر. تم العثور على Ag NPs المركب من *E.tef* و *V. paradoxa* بقطر 12.59 – 34.60 نانومتر ، 29.05 – 83.94 نانومتر على التوالي. وجد أن النتيجة المضادة للبكتيريا ضد مسببات الأمراض التجريبية تتراوح من 12–22 مم و 13–19 مم باستخدام Ag NPs من مستخلصات بذور *E. tef* و *V. paradoxa* على التوالي. بالإضافة إلى ذلك ، أظهرت النتائج أن هناك تأثير واضح على *Acinetobacter baumannii* من عزلات مياه الصرف الصحي بالمستشفى. كان التأثير السام لـ Ag NPs ضد الخلايا السرطانية 77.12 (كان تركيز Ag NPs هو 75٪) من *E.tef* و 77.23 (تركيز Ag NPs كان 50٪) من *V. paradoxa*.

الكلمات المفتاحية: مضاد للسرطان، تخليق أخضر، بكتيريا ممرضة، نترات الفضة.